

**Formation of Fe<sub>3</sub>O<sub>4</sub>@MnO<sub>2</sub> ball-in-ball hollow spheres as a high performance catalyst for enhanced catalytic performances**

Shouwei Zhang<sup>a</sup>, Qiaohui Fan<sup>b</sup>, Huihui Gao<sup>a</sup>, Yongshun Huang<sup>c</sup>, Xia Liu<sup>c</sup>, Jiaxing Li<sup>\*c,d</sup>, Xijin Xu<sup>\*a</sup>,  
Xiangke Wang<sup>\*d</sup>

<sup>a</sup> School of Physics and Technology, University of Jinan, Shandong, 250022, P. R. China.

<sup>b</sup> Key Laboratory of Petroleum Resources, Gansu Province/Key Laboratory of Petroleum Resources Research, Institute of Geology and Geophysics, Chinese Academy of Sciences, Lanzhou 730000, P.R. China

<sup>c</sup> Key Laboratory of Novel Thin Film Solar Cells, Institute of Plasma Physics, Chinese Academy of Sciences P.O. Box 1126, 230031 Hefei, P. R. China Tel: +86-551-65596617,

<sup>d</sup> NAAM Research Group, Faculty of Science, King Abdulaziz University, Jeddah 21589, Saudi Arabia.

Corresponding authors: E-mail: lijx@ipp.ac.cn(J. Li), Tel: +86-551-65596617

### **Preparation of hierarchical MnO<sub>2</sub> hollow/solid spheres**

*MnO<sub>2</sub> hollow spheres*<sup>1</sup>: SiO<sub>2</sub> spheres (200 mg) into 0.01 M KMnO<sub>4</sub> (70 mL) solution under stirring. Subsequently, the mixture was transferred to a 100 mL autoclave and kept at 160 °C for 12 h. After the autoclave was cooled to room temperature, the product was etched by 2 M NaOH to remove the SiO<sub>2</sub> core. The final products, the hierarchical MnO<sub>2</sub> hollow spheres were obtained after centrifugation and washed by deionized water.

*MnO<sub>2</sub> solid spheres*: The MnO<sub>2</sub> solid sphere was prepared using similar methods without the presence of SiO<sub>2</sub> spheres.

### **Preparation of Fe<sub>3</sub>O<sub>4</sub> hollow/solid spheres**

*Fe<sub>3</sub>O<sub>4</sub> hollow spheres*<sup>2</sup>: In a typical synthesis of hierarchical Fe-glycerate hollow spheres, Fe(NO<sub>3</sub>)<sub>3</sub>·6H<sub>2</sub>O (0.202 g) and glycerol (7.5 mL) were added into isopropanol (52.5 mL). After stirring for 5 min, 1 mL of deionized water was added into the above solution. After stirring for another 10 min, the container was then transferred to a stainless steel autoclave and kept in an electrical oven at 190 °C for 12 h. After cooling to room temperature naturally, the precipitate was separated by centrifugation, washed with several times with ethanol and dried in an oven at 70 °C overnight, and then annealed at 350 °C for 3 h in N<sub>2</sub>.

*Fe<sub>3</sub>O<sub>4</sub> solid spheres*<sup>3</sup>: FeCl<sub>3</sub>·6H<sub>2</sub>O (1.35 g) was dissolved in ethylene glycol (40 mL) to form a clear solution, followed by the addition of NaAc (3.6 g) and polyethylene glycol (1.0 g). The mixture was stirred vigorously for 30 min and then sealed in 50 mL autoclave. The autoclave was heated to and maintained at 200 °C for 24 h, and allowed to cool to room temperature. The black products were washed several times with ethanol and dried at 60 °C for 6 h.

### **Catalytic degradation procedure**

Methylene blue (MB) degradation was performed in a 250 mL conical flask with MB (30 mg/L) solution and dipped in a constant-temperature water bath (298 K). The catalysts (300 mg/L) was first added to the solution and stirred for 120 min and then PMS (20 mM) was added to the solution to start the degradation.

Solution pH was adjusted by 0.01 M H<sub>2</sub>SO<sub>4</sub> or NaOH. At defined time intervals, an aliquot of 3 mL solution was withdrawn by a syringe, which was immediately quenched by ethanol (3 mL). The catalysts were separated using magnet, and the concentration of MB ( $\lambda=664$  nm) was determined using a UV-vis spectrometer. The effects of foreign ions (Cl<sup>-</sup>, NO<sub>3</sub><sup>-</sup>, SO<sub>4</sub><sup>2-</sup>, ClO<sub>4</sub><sup>-</sup>, Na<sup>+</sup>, K<sup>+</sup>, Ca<sup>2+</sup>) at 0.1 M on the degradation reaction were studied. The experiments were carried out under the same reaction conditions with MB (30 mg/L), PMS (20 mM), pH~7.98 and the used catalysts (300 mg/L) at 298 K. Various model pollutants (victoria blue B (VB), rhodamine B (RhB), methyl orange (MO), phenol and methyl violet (MV)) at 30 mg/L on the degradation reaction were studied. The experiments were carried out under the same reaction conditions with PMS (20 mM), pH~7.98 and the used catalysts (300 mg/L) at 298 K. In addition, two sets of quenching tests were carried out to determine the radical species formed in the catalytic system by using *tert*-butyl alcohol (TBA) and ethanol as the radical scavengers.

For the kinetic rates of dye degradation, the pseudo-first order kinetic was employed,<sup>4</sup>

$$-\frac{d[MB]}{dt} = k_{obs}[MB]$$

where  $[MB]_0$  (mg/L) and  $[MB]$  (mg/L) are the MB concentrations at time 0 and at any specific time  $t$ , respectively; and  $k_{obs}$  is the pseudo-first-order degradation rate constant ( $\text{min}^{-1}$ ).

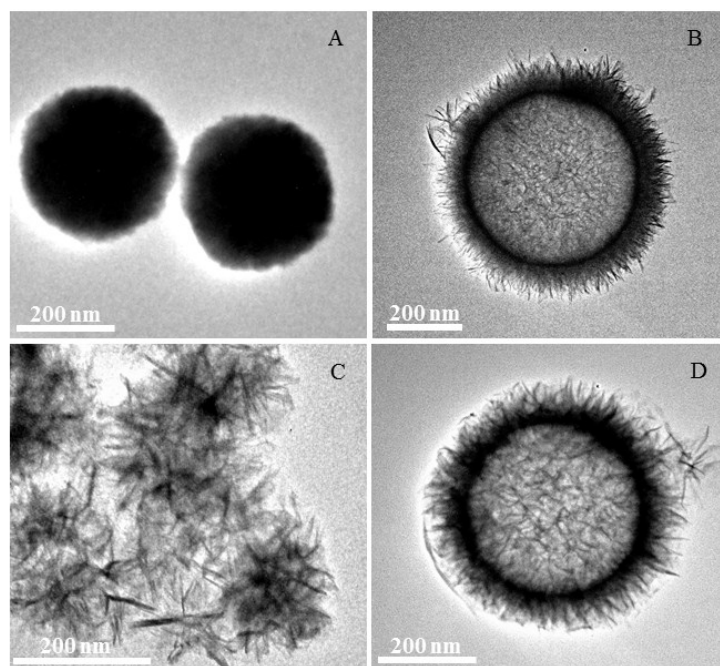


Figure S1. The TEM images of  $\text{Fe}_3\text{O}_4$  solid/hollow spheres (A and B) and hierarchical  $\text{MnO}_2$  hollow/solid spheres (C and D)

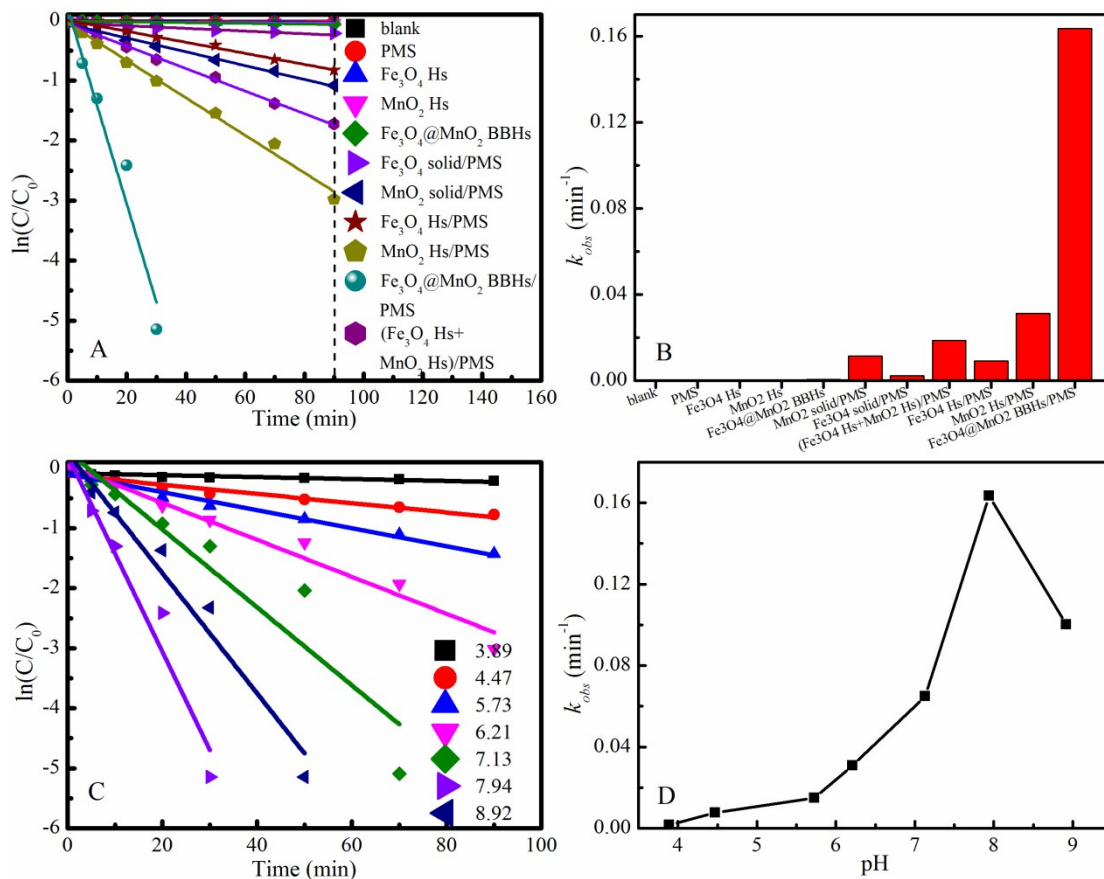


Figure S2. The pseudo-first order kinetic of MB degradation onto the different catalysts (A and B) and pH (B and C).

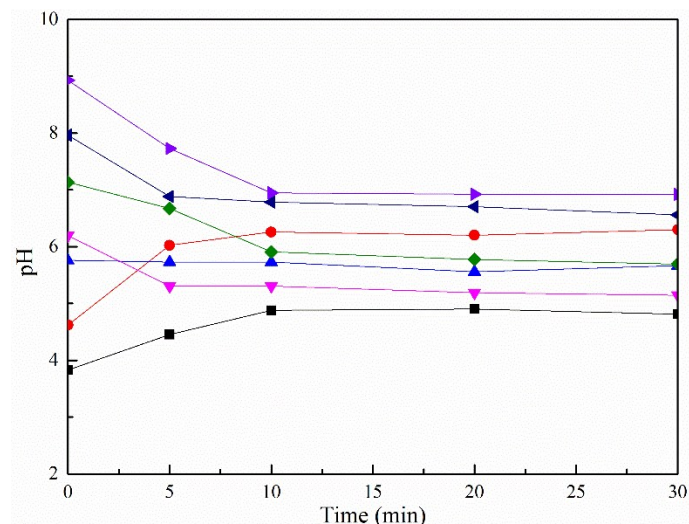


Figure S3. pH variation during the reaction in the Fe<sub>3</sub>O<sub>4</sub>@MnO<sub>2</sub> BBHs system.

Figure 1 shows that the final pH values remain ~4.8~6.9 after ~30 min probably due to the buffering ability of the catalyst. Moreover, for low initial pH, the rise of initial pH is also beneficial for the formation of surface hydroxyl groups on the catalyst, which can behave as an active site for electron transfer and thus improve the performance of the catalyst.

The pH was set at initial. The surface charge of metal oxides is highly dependent on the relation between solution pH and p<sub>H</sub>pzc of metal oxides. At pH < p<sub>H</sub>pzc, the surface charge of metal oxides is positive while negative at pH > p<sub>H</sub>pzc. On the other hands, the existed form of PMS was HSO<sub>5</sub><sup>-</sup> at acid and neutral condition and SO<sub>5</sub><sup>2-</sup> at pH 9.5. The p<sub>H</sub>pzc of Fe<sub>3</sub>O<sub>4</sub>@MnO<sub>2</sub> BBHs was determined as ~8.1. Thus, at pH 9.5, the interaction between negative charged surface and SO<sub>5</sub><sup>2-</sup> is reduced due to the formation of repulsive force. Additionally, PMS is unstable at basic pH and can be self-decomposed mainly through non-radical route with a maximum decomposition rate at the pH value equal to its second pK<sub>a</sub> (~9.4). Both of the reasons lead to the decline of the MB degradation efficiency while enhancement of the MB degradation at pH < 8.1. In the Fe<sub>3</sub>O<sub>4</sub>@MnO<sub>2</sub> BBHs/PMS system, the MB degradation efficiency was declined as the pH increased from ~7.94 to ~8.92, revealing the electrostatic factors and self-decomposition of HSO<sub>5</sub><sup>-</sup> through non-radical route controlled the generation of the sulfate radicals. However, the MB degradation efficiency was declined as the pH decreased from ~7.94 to ~3.89 rather than enhanced. The lower rate of MB degradation at this pH might be attributed to the relatively higher

stability of the oxidant at acidic pH values that could reduce the generation of radicals. Besides, in acidic condition, the formation of H-bond between  $H^+$  and the O-O group of  $HSO_5^-$  would be more significant that decrease the positive charge of  $HSO_5^-$ , thus hindering the interaction between  $HSO_5^-$  and the catalyst surface.



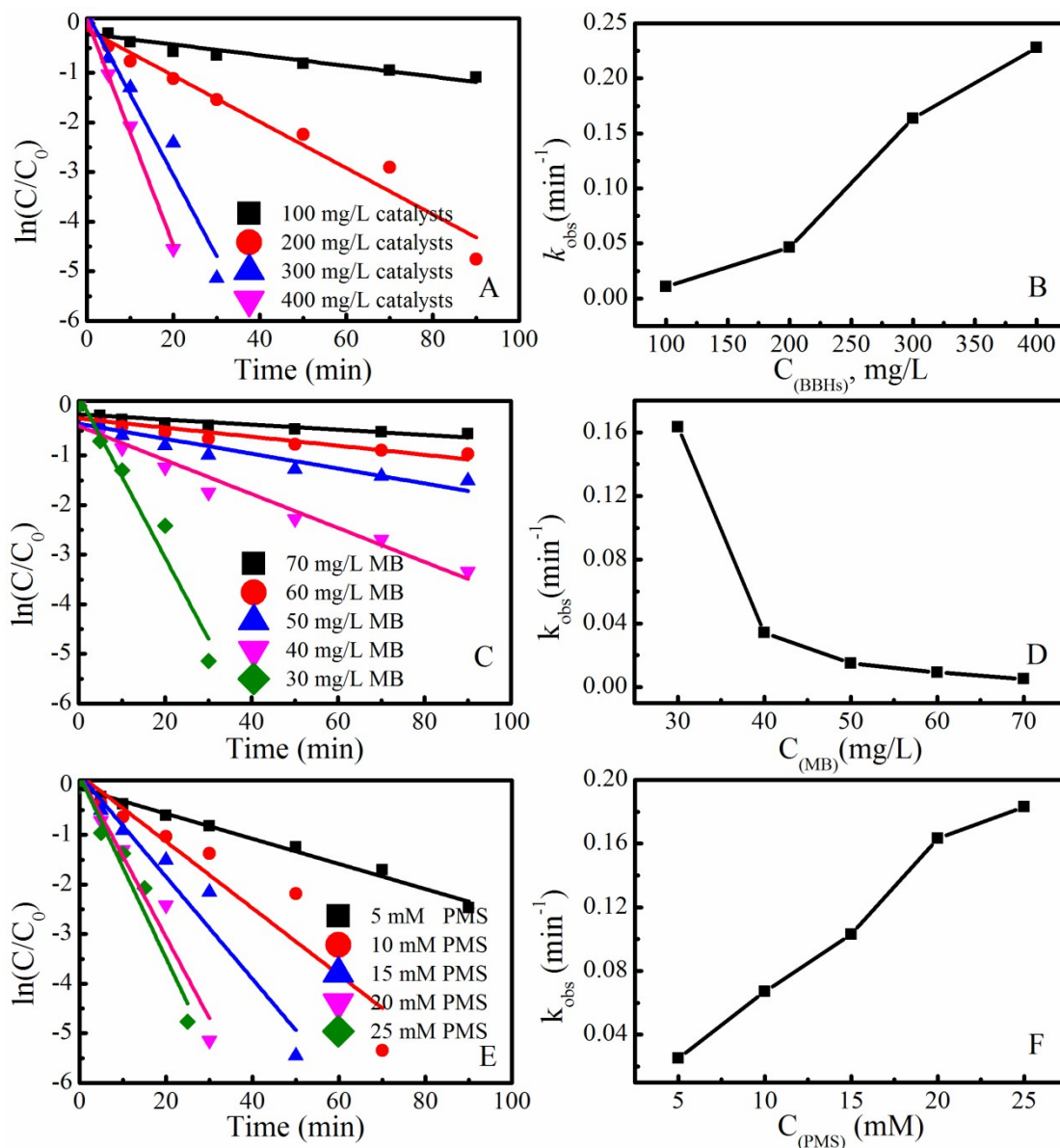


Figure S4. The pseudo-first order kinetic of MB degradation onto the  $\text{Fe}_3\text{O}_4@\text{MnO}_2$  BBHs under different condition: catalyst loading (A and B), MB concentration (C and D) and PMS concentration (E and F).

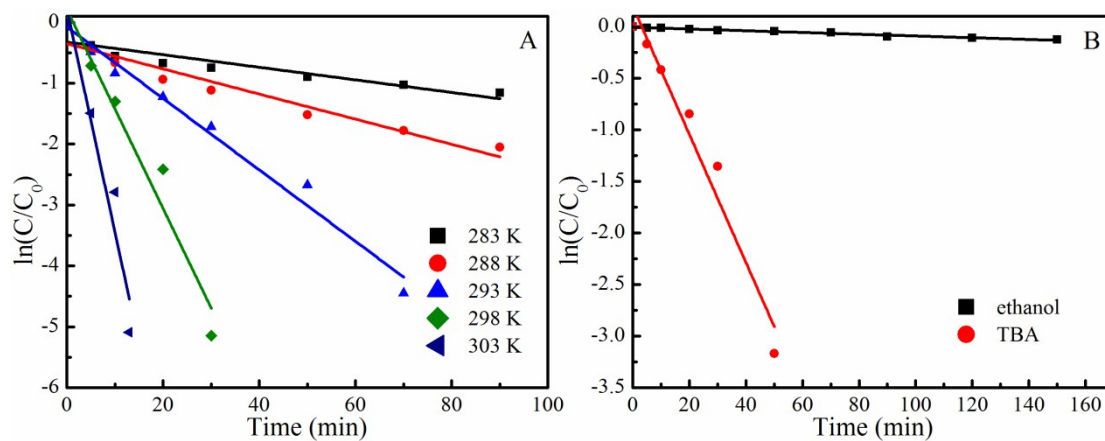


Figure S5. The pseudo-first order kinetic of MB degradation onto the  $\text{Fe}_3\text{O}_4@\text{MnO}_2$  BBHs under different temperature (A) and radical scavengers (B).

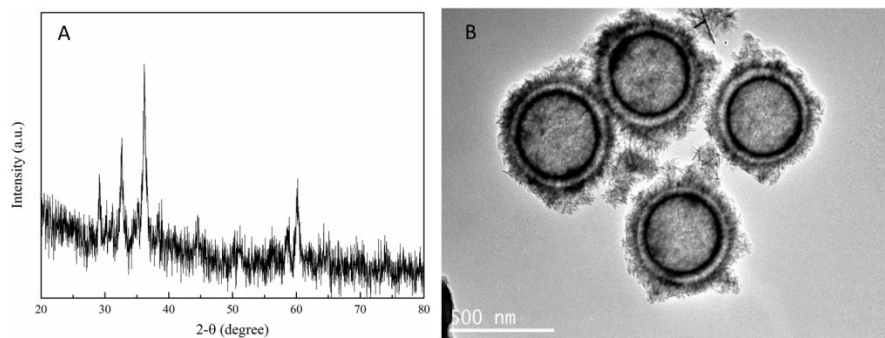


Figure S6. The XRD and TEM results revealed that the hierarchical ball in ball hollow structures and crystalline of the recovered catalyst was scarcely changed.

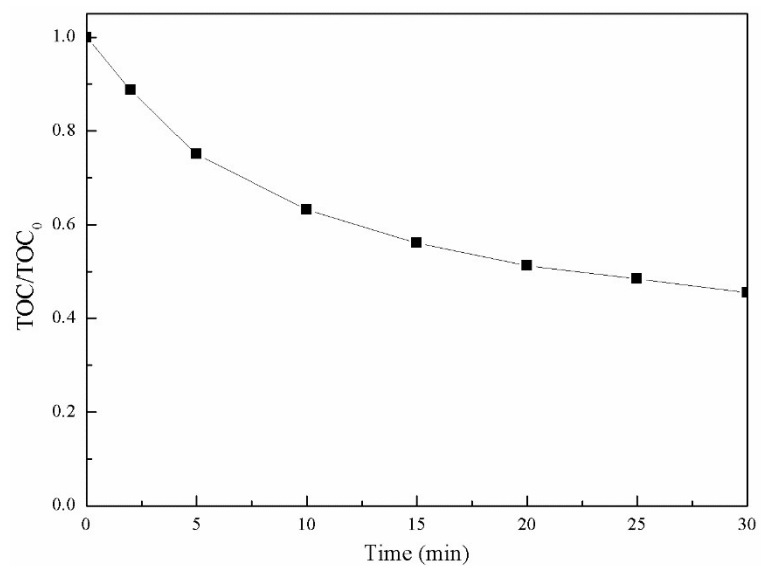


Figure S7. TOC removal during the degradation of MB.

Table S1. The pseudo first-order rate constant ( $k_{obs}$ ) of the degradation of MB under different pH using PMS activated by different catalysts

Catalysts (30 mg/L)	MB (mg/L)	PMS (mM)	T (K)	pH	$k_{obs}$ (min <sup>-1</sup> )	$R^2$	
blank	30	0	298	7.94	0.00002	0.939	
PMS		20			0.00008	0.986	
Fe <sub>3</sub> O <sub>4</sub> Hs		0			0.0002	0.941	
MnO <sub>2</sub> Hs					0.0003	0.955	
Fe <sub>3</sub> O <sub>4</sub> @MnO <sub>2</sub> BBHs		20			20	0.0006	0.953
Fe <sub>3</sub> O <sub>4</sub> solid sphere						0.0022	0.912
MnO <sub>2</sub> solid sphere						0.0115	0.989
Fe <sub>3</sub> O <sub>4</sub> Hs+ MnO <sub>2</sub> Hs						0.0187	0.976
Fe <sub>3</sub> O <sub>4</sub> Hs						0.0092	0.996
MnO <sub>2</sub> Hs						0.0312	0.995
Fe <sub>3</sub> O <sub>4</sub> @MnO <sub>2</sub> BBHs						0.1634	0.943
Fe <sub>3</sub> O <sub>4</sub> @MnO <sub>2</sub> BBHs		30			20	298	3.89
	4.47		0.0077	0.932			
	5.73		0.0149	0.982			
	6.21		0.0308	0.968			
	7.13		0.0649	0.921			
	7.94		0.1634	0.943			
	8.92		0.1001	0.961			

Table S2. The pseudo first-order rate constant ( $k_{obs}$ ) of the degradation of MB under different conditions using PMS activated by Fe<sub>3</sub>O<sub>4</sub>@MnO<sub>2</sub> BBHs.

Fe <sub>3</sub> O <sub>4</sub> @MnO <sub>2</sub> BBHs (mg/L)	MB (mg/L)	PMS (mM)	T (K)	Inhibitor	pH	$k_{obs}$ (min <sup>-1</sup> )	$R^2$
100	30	20	298	-	7.94	0.0108	0.922
200						0.0466	0.963
300						0.1634	0.943
400						0.2279	0.996
300	70	20	298			0.0052	0.866
	60					0.0091	0.921
	50					0.0151	0.942
	40					0.0342	0.954
	30					0.1634	0.963
300	30	5	298			0.0253	0.998
		10				0.0671	0.928
		15				0.1032	0.935
		20				0.1634	0.943
		25				0.1832	0.944
300	30	20	283			0.0103	0.896
			288			0.0207	0.922
			293	0.0587	0.978		
			298	0.1634	0.943		
			303	0.3666	0.986		
300	30	20	298	ethanol	0.0008	0.969	
				TBA	0.0624	0.955	

## References

1. X. Tang, Z.-h. Liu, C. Zhang, Z. Yang and Z. Wang, *J. Power Sources*, 2009, **193**, 939-943.
2. F. X. Ma, H. Hu, H. B. Wu, C. Y. Xu, Z. Xu and L. Zhen, *Adv. Mater.*, 2015, **27**, 4097-4101.
3. H. Deng, X. Li, Q. Peng, X. Wang, J. Chen and Y. Li, *Angew. Chem. Int. Edit.*, 2005, **117**, 2842-2845.
4. C. Tan, N. Gao, Y. Deng, J. Deng, S. Zhou, J. Li and X. Xin, *J. Hazard. Mater.*, 2014, **276**, 452-460.